



Article

Triiron Tetrairon Phosphate ($\text{Fe}_7(\text{PO}_4)_6$) Nanomaterials Enhanced Flavonoid Accumulation in Tomato Fruits

Zhenyu Wang^{1,2}, Xiehui Le^{1,2}, Xuesong Cao^{1,2}, Chuanxi Wang^{1,2}, Feiran Chen^{1,2}, Jing Wang^{1,2}, Yan Feng^{1,2}, Le Yue^{1,2,*} and Baoshan Xing³

- ¹ School of Environment and Civil Engineering, Institute of Environmental Processes and Pollution Control, Jiangnan University, Wuxi 214122, China; wang0628@jiangnan.edu.cn (Z.W.); 6191403013@stu.jiangnan.edu.cn (X.L.); caoxuesong@jiangnan.edu.cn (X.C.); wangcx2018@jiangnan.edu.cn (C.W.); chenfeiran@jiangnan.edu.cn (F.C.); wangjing03282022@163.com (J.W.); 15251870663@163.com (Y.F.)
- ² Jiangsu Engineering Laboratory for Biomass Energy and Carbon Reduction Technology, Wuxi 214122, China
- ³ Stockbridge School of Agriculture, University of Massachusetts, Amherst, MA 01003, USA; bx@umass.edu
- * Correspondence: leyue@jiangnan.edu.cn; Tel.: +86-0510-85911911

Abstract: Flavonoids contribute to fruit sensorial and nutritional quality. They are also highly beneficial for human health and can effectively prevent several chronic diseases. There is increasing interest in developing alternative food sources rich in flavonoids, and nano-enabled agriculture provides the prospect for solving this action. In this study, triiron tetrairon phosphate ($\text{Fe}_7(\text{PO}_4)_6$) nanomaterials (NMs) were synthesized and amended in soils to enhance flavonoids accumulation in tomato fruits. 50 mg kg⁻¹ of $\text{Fe}_7(\text{PO}_4)_6$ NMs was the optimal dose based on its outstanding performance on promoting tomato fruit flavonoids accumulation. After entering tomato roots, $\text{Fe}_7(\text{PO}_4)_6$ NMs promoted auxin (IAA) level by 70.75 and 164.21% over Fe-EDTA and control, and then up-regulated the expression of genes related to PM H⁺ ATPase, leading to root proton ef-flux at 5.87 pmol cm⁻² s⁻¹ and rhizosphere acidification. More Mg, Fe, and Mn were thus taken up into plants. Subsequently, photosynthate was synthesized, and transported into fruits more rapidly to increase flavonoid synthesis potential. The metabolomic and transcriptomic profile in fruits further revealed that $\text{Fe}_7(\text{PO}_4)_6$ NMs regulated sucrose metabolism, shi-kimic acid pathway, phenylalanine synthesis, and finally enhanced flavonoid biosynthesis. This study implies the potential of NMs to improve fruit quality by enhancing flavonoids synthesis and accumulation.

Keywords: flavonoids; tomato fruits; $\text{Fe}_7(\text{PO}_4)_6$ NMs; transcriptomic; metabonomic



Citation: Wang, Z.; Le, X.; Cao, X.; Wang, C.; Chen, F.; Wang, J.; Feng, Y.; Yue, L.; Xing, B. Triiron Tetrairon Phosphate ($\text{Fe}_7(\text{PO}_4)_6$) Nanomaterials Enhanced Flavonoid Accumulation in Tomato Fruits. *Nanomaterials* **2022**, *12*, 1341. <https://doi.org/10.3390/nano12081341>

Academic Editors: Marta Marmiroli and Elena Maestri

Received: 24 February 2022

Accepted: 7 April 2022

Published: 13 April 2022

Publisher's Note: MDPI stays neutral with regard to jurisdictional claims in published maps and institutional affiliations.



Copyright: © 2022 by the authors. Licensee MDPI, Basel, Switzerland. This article is an open access article distributed under the terms and conditions of the Creative Commons Attribution (CC BY) license (<https://creativecommons.org/licenses/by/4.0/>).

1. Introduction

Flavonoids, a kind of C6-C3-C6 skeleton phenolic secondary metabolite, play an important role in food organoleptic properties and human health [1]. For example, flavonoids are able to protect cells from oxidative stress [2], regress tumors [3], regulate diabetes and obesity [4], alleviate inflammation, and enhance the immune system [5]. Bondonno et al. (2019) [6] reported that the habitual intake of flavonoids could decrease cardiovascular and cancer induced mortality and recommend humans to increase the intake of flavonoid-rich foods. However, the flavonoids intake of populations has remained low due to eating habits involving flavonoids-lacking foods. Therefore, there is increasing interest in developing alternative food sources rich in flavonoids [7]. Tomatoes (*Solanum lycopersicum* L.), including a wide variety of processed tomato food products (e.g., ketchup, pasta sauce, and tomato puree), are one of the major vegetables in human diets and are therefore an ideal candidate for improved flavonoids intake [8].

To date, nano-enabled agriculture technology is emerging for crop yield and quality improvement. Recent studies discovered that flavonoids could be enhanced with nanomaterials (NMs) applications. For example, 10 mg/L Se and Cu NMs significantly enhanced the

content of flavonoids in tomato fruits by 26.4 and 20.9% as compared with control [9]. The application with 250 mg/L SiO₂ NMs also significantly increased the flavonoids content in tomato fruits [10]. Given these promising findings and the known importance of flavonoids in tomato fruits, future investigation into the mechanisms of action and optimization of efficacy is warranted.

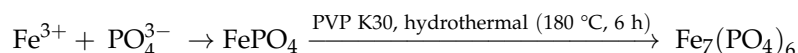
The synthesis of flavonoids in plants is highly regulated by sucrose, which can act as a signaling molecule to affect flavonoid synthesis related genes expression [11–13]. In addition, sucrose could activate phenylpropanoid metabolism, which leads to flavonoid synthesis and upregulate the expression of transcription factors (TFs) like *bHLH1*, *MYB* and *WD40* [14,15]. *bHLH* TFs can positively regulate the synthesis of flavonoids [16]. *MYB* TFs can increase the expression of chalcone synthase, chalcone isomer and other enzyme genes in the flavonoids metabolic process [17]. *WD40* is not considered to have any catalytic activity alone, but they act as a bridge combining *MYB* and *bHLH* to form a complex in regulating flavonoid synthesis [18]. Therefore, enhancing the sucrose accumulation in tomato fruits could effectively increase their flavonoids content. It should be noted that sucrose in tomato fruits mainly comes from photosynthetic carbon fixation [19]. The photosynthetic system requires the participation of various elements (e.g., Fe, Mn, and P). However, these elements present low bioavailability in the soil, and plants usually adopt the strategy of acidifying the rhizosphere to obtain them [20]. Plasma membrane (PM) H⁺-ATPase facilitates the transport of various nutrients, such as nitrate, phosphate and potassium, and is responsible for pumping protons out of the plasma to achieve acidification [21,22]. The overexpression of PM H⁺-ATPase could increase rice yield through simultaneous enhancement of photosynthesis and nutrient uptake [23,24]. Besides, Fe and P play a vital role in plant growth [25,26]. Fe was a key element for 2-oxoglutarate dependent (2-ODD) oxygenases that oxidize the central C ring in flavonoid synthase. Therefore, materials such as composite triiron tetrairon phosphate (Fe₇(PO₄)₆) are of particular interest for application as part of a nano-enabled strategy to elevate flavonoids accumulation in tomato fruits. Interestingly, several studies mentioned that Fe-based NMs could induce the activation of root PM H⁺-ATPase [23,27]. In the present study, we hypothesized that tomato roots exposed to Fe₇(PO₄)₆ NMs in soil could trigger high activity of PM H⁺-ATPase to acidify rhizosphere in order to mobilize nutrient elements and promote photosynthesis, more sucrose would accumulate and induce flavonoids biosynthesis in tomato fruits. The goal of this work was to investigate the mechanisms of enhanced flavonoid accumulation in tomato fruits by the amendment with Fe₇(PO₄)₆ NMs, including: (1) PM H⁺-ATPase activity in tomato seedling roots; (2) nutrient uptake, photosynthesis, and sucrose accumulation during the plant growth; and (3) flavonoid synthesis in tomato fruits by the metabolomic and transcriptomic profiles. This study highlights the potential of NMs to improve human health through elevating flavonoid accumulation in dietetic fruits.

2. Materials and Methods

2.1. Synthesis and Characterization of Fe₇(PO₄)₆ NMs

The chemicals for NM synthesis were all purchased from Sinopharm Chemical Reagent Co., Ltd, Shanghai, China. Pristine Fe₇(PO₄)₆ NMs were synthesized based on the study of Song et al. (2015) [28] with slight modification. Firstly, 3.45 g NH₄H₂PO₄ was dissolved in 20 mL deionized (DI) water at 25 °C, making a 173 mg L⁻¹ NH₄H₂PO₄ solution. In order to produce nanoscale suspended particles, 0.5 g PVP-K30 (Polyvinylpyrrolidone K30) was dissolved in 10 mL DI water, and then mixed with the above NH₄H₂PO₄ solution. Then, 2.025 g FeCl₃·6H₂O was dissolved in 20 mL DI water, making a 101 mg L⁻¹ ferrous solution. Then, the ferrous solution was added dropwise for 6 s per drop into the PVP-K30 and NH₄H₂PO₄ mixture with a magnetic stirrer until all ferrous solution was consumed. Afterwards, the obtained mixture was centrifuged at 6000 rpm for 10 min and the supernatant was discarded. The precipitate was transferred into a 100 mL Teflon-lined stainless steel autoclave. The autoclave was sealed and heated to 180 °C for 6 h. After taking out and cooling down, the products were separated by centrifugation at 5000 rpm for 5 min

and washed by DI water for three times. After dried in vacuum oven at 60 °C for 2 h, Fe₇(PO₄)₆ NMs were obtained. The productivity of synthetic Fe₇(PO₄)₆ NMs was 0.92 g. The chemical reaction is shown below:



The shape and size of synthesized Fe₇(PO₄)₆ NMs were observed by transmission electron microscopy (TEM, JEM-2100, Nippon electronics Co., Tokyo, Japan). Energy dispersive spectroscopy (EDS) was used for Fe, P and O qualitative analysis. The chemical formula composition was examined by X-ray diffraction (XRD, Bruker AXS, Berlin, Germany) and Jade 5 was performed for peak detection. X-ray photoelectron spectroscopy (XPS, Thermo Fisher ESCALAB 250Xi, Waltham, MA, USA) was applied to test Fe valence of Fe₇(PO₄)₆ NMs and Avantage 5.9 (Thermo Fisher, Waltham, MA, USA) was used for data analysis. Zetasizer (Nano-ZS90, Malvern Instruments, Malvern, UK) was used to examine the surface charge (zeta potential) and hydrodynamic diameter (Dh) of the Fe₇(PO₄)₆ NM suspension.

2.2. Plant Cultivation and NM Exposure

Tomato seeds (*Solanum lycopersicum* L., No. 1 Jinpeng, Xi'an Jinpeng seed Co., Ltd., Xian, China) were chosen with similar size, sterilized with 5% NaClO for 10 min, and thoroughly washed with DI water three times. The sterilized seeds were soaked in DI water for 4 h and then laid flat on totally wet filter paper and incubated in darkness at 25 °C for 48 h to germinate. After that, the tomato seedlings of uniform size and degree of germination were transferred to soil homogenized with Fe₇(PO₄)₆ NMs in pots for seedling and fruit experiments.

Fe₇(PO₄)₆ NMs were mixed with soil vigorously to guarantee that soil was homogenized with the NMs thoroughly before tomato seedling cultivation. The soil was collected from a farm located in Wuxi (latitude 31.52° N and longitude 120.13° E, China) and the properties of soil are shown in Table S1. 600 g amended soil in each pot was used in seedling experiment and the plants were harvest after 42 days of cultivation. 4 kg amended soil in each pot was used in a fruit experiment and tomato fruits were collected after 115 days cultivation. Wang et al. (2020) [29] concluded that the impacts of NMs on crop growth exhibited a trend of low-promoting and high-inhibiting. Fe-based NMs shows increasing positive effects trend with the concentration (<50 ppm), but positive trend decreased if NMs concentration was more than 50 ppm. Thus, 50 mg kg⁻¹ of Fe₇(PO₄)₆ NMs was selected for enhancing plant growth, and 5 ppm was chosen to be set as comparison to 50 ppm.

The plants were grown under greenhouse conditions, with temperatures of 28/20 °C for day and night, and a relative humidity of 60%. Each pot was set as a biological replicate, and each treatment contained six replicates. In the seedling experiment, each pot retained two seedlings to gain enough biomass for tests. As for fruit experiments, one seedling was cultured in each pot. 5 and 50 mg kg⁻¹ were set in a preliminary experiment to explore their impacts on flavonoid accumulation. The results indicated that 50 mg kg⁻¹ Fe₇(PO₄)₆ NMs better promoted flavonoid content in fruits; therefore, 50 mg kg⁻¹ Fe₇(PO₄)₆ NMs was used in the following experiments. Fe-EDTA considered as commercial Fe fertilizer, which contained equivalent mass of Fe (20.4 mg kg⁻¹) with 50 mg kg⁻¹ Fe₇(PO₄)₆ NMs, was mixed in the same way as NMs and was also conducted in the seedling experiments. "CK" was defined as control.

2.3. Photosynthesis, Root Parameters, Element Content, and Single Particle Concentration

The relative chlorophyll content of tomato leaves was measured by Chlorophyll Meter (SPAD-502 Plus, Konica Minolta Inc., Tokyo, Japan) when the tomato grew to the fourth leaf stage (the fourth true leaf was fully unfolded). Net photosynthetic rate (Pn), stomatal conductance (Gs), transpiration rate (E), and intercellular CO₂ concentration (Ci) were measured by CIRAS-3 portable gas exchange system (CIRAS-3, PP-Systems, Amesbury, MA,

USA). The root morphology was scanned by WinRHIZO Pro 2017 b (Regent Instruments Inc., Ville de Québec, Quebec, Canada).

For the determination of nutrient content, 25 mg oven-dried tomato shoots and roots of fourth leaf stage (six replicates) were added into a digestion tube with 3 mL ultra-pure water and 3 mL nitric acid successively, and put into the digestion apparatus (MARS 6, CEM, Matthews, NC, USA), then the digestion was carried out at 190 °C, 1400 W. After digestion, the liquid was filtered by a 0.22 µm filter and diluted to 50 mL. The protocol of sample treatments was based on Wang et al. (2021) [30] with modifications. 25 mg of the tissue in fourth leaf stage was washed three times with DI water and then homogenized in 3 mL 20 mM 2-(*N*-morpholino) ethanesulfonic acid (MES) buffer (pH = 5.0). Then, the mixture was shaken at 37 °C for 24 h. After centrifugation at 12,000 rpm for 5 min, the supernatant was collected and taken through 0.45 µm filter membrane. The leachate was double diluted with DI water before single particle test. The content of Fe₇(PO₄)₆ NMs in plant shoots, roots, and stems was determined by single particle ICP-MS (SP-ICP-MS, Thermo Fisher, Bremen, Germany) and parameters setting of testing were referred to Xu et al. (2020) [31].

2.4. Net H⁺ Flow Rate, IAA Content and Flavonoid Content

The protocol of net H⁺ flow rate determination was based on Ye et al. (2021) [32] and performed on Non-invasive Micro-test Technology System (NMT, 100S-SIM-XY, Xuyue Sci & Tech Co., Ltd., Beijing, China). The H⁺ microsensors were prepared as follows: a microsensor (Φ4.5 ± 0.5 µm, XY-CGQ-01, Xuyue, China) was placed 1 cm from the tip and filled with H⁺ exchange liquid (15 mM NaCl, 40 mM KH₂PO₄, pH = 7.0). Then, the microsensor was filled with H⁺ exchange reagent (LIXs, XY-SJ-H-10, Xuyue Sci & Tech Co., Ltd., Beijing, China). Before measuring H⁺ flow, the microsensors were calibrated with H⁺ calibration solutions (0.1 mM CaCl₂, pH = 5.5 and pH = 6.5) and kept Nernst slope at 58 ± 5 mV decade⁻¹. The tomato seedlings of fourth leaf stage were washed with DI water and the roots were completely immersed in test solution (0.1 mM CaCl₂, 0.3 mM 2-(*N*-morpholino) ethanesulfonic acid, pH = 6) for 30 min of equilibration. The intact roots were selected on the Non-invasive Micro-test Technology System (NMT, 100S-SIM-XY, Xuyue Sci & Tech Co., Ltd., Beijing, China). The intact and unbroken roots were selected under the microscope and initial position of microsensor tip was set at 5 µm from the root surface. The root elongation region was selected as the probe detection region [33–35]. The step size of the probe was set to 20 µm, and the H⁺ flow rate was collected every 4 s. The data processing was performed by imFluxes V2.2 software.

IAA content determination was performed on Ultra performance liquid chromatography coupled with electrospray ionization and mass spectrometry (UPLC-ESI-MS/MS) based on the studies of Xiao et al. (2019) [36]. In brief, 100 mg from fourth leaf stage was ground in liquid nitrogen and added with 1 mL ethyl acetate, including 10 µg mL⁻¹ butylated hydroxytoluene. After vortexing for 15 min, the samples were ultrasonically extracted in ice for 15 min. After centrifugation at 4 °C, 12,000 rpm for 10 min, the supernatant was transferred into a new tube and gently evaporated to dryness under nitrogen flow. The residual was redissolved in 200 µL 70% ethanol (*v/v*), 10 µL of the solution was directly injected in UPLC-ESI-MS/MS. UPLC-ESI-MS/MS equipment system setup was described in Text S1. The methods of flavonoid extraction and detection were described in Text S2.

2.5. Sucrose Content in Fruits

The method of sucrose content in tomato fruits was measured based on Feng et al. (2019) with slight modifications [37]. Dried samples were homogenized with 3 mL of 80% (*v/v*) ethanol and heated to 80 °C in water bath for 10 min; the sediment was collected by centrifugation at 8000 rpm for 10 min. The extraction process was carried out another three times as described above, and supernatant was collected each time. Next, 10 mg activated carbon was added to supernatant for decoloring and 0.1 mL of 0.1 M NaOH solution was added into 0.9 mL of supernatant. 3 mL of 10 M HCl and 1 mL of 0.1% resorcinol

solution (0.1 g of resorcinol with 100 mL of 95% ethanol) were added to the supernatant in 80 °C water bath for 30 min. After the supernatant cooling down to room temperature, the sucrose concentration was determined using a microplate reader (Thermo Scientific, Waltham, MA, USA) at 480 nm.

2.6. Quantitative Real-Time PCR (qRT-PCR)

Gene expressions of flavonoid synthesis related genes (*SIPAL*, *SIC4H*, *SI4CL*, and *SICHI*) in fruits and PM H⁺ ATPase (*LHA1*, *LHA2*, and *LHA4*) in roots were determined. Sucrose transporter related genes of *SISUT1*, *SISUT2*, and *SISUT4* were examined in seedling leaves. The sequences of primers of internal reference gene and other target ones were listed in Table S2. The plant samples were ground into powder in liquid nitrogen. According to plant RNA extraction protocol (TaKaRa MiniBEST Plant RNA Extraction Kit), total RNA of roots and fruits was isolated, which was used as templates to proceed reverse transcription using T100 Thermal Cycler (Bio-Rad, Hercules, CA, USA). The reverse transcription procedure was carried out with EasyQuick RT MasterMix (CW BIO) kit and the conditions was as follow: 37 °C for 15 min, 85 °C for 5 s, and stored at 4 °C to obtain cDNA for PCR (polymerase chain reaction). Real-time PCR was executed with UltraSYBR Mixture (CW BIO) as fluorochrome operating on a CFX96 Real-Time system combined with C1000 Touch Thermal Cycler (Bio-Rad, Hercules, CA, USA). The targeted DNA amplification procedure was set as follows: (1) pre-degeneration at 95 °C for 10 min, (2) denaturation at 95 °C for 15 s, followed by (3) 60 °C for 1 min, and a total of 40 cycles of (2) to (3) were performed. The standard calculation $2^{-\Delta\Delta CT}$ was used to measure the relative expression of the targeted genes [38].

2.7. Transcriptomic and Metabolomic Analysis of Tomato Fruits

Transcriptomic analysis of tomato fruits was performed by Genedenovo Biotechnology Co., Ltd. (Guangzhou, China). Briefly, the expression level of each gene was measured by fragments per kilobases per millionreads (FPKM). The differences in RNA expressions were analyzed by DESeq2, DEGseq and edgeR. The systematic analysis of gene function was conducted by comparison to the Kyoto Encyclopedia of Genes and Genomes (KEGG) and Gene ontology (GO) databases.

The extraction, identification, and quantification of tomato metabolites were conducted according to García et al. (2017) [39]. A one hundred microgram fruit sample was put in 2 mL tubes, and was mixed with 1.5 mL methanol/water (80:20, *v/v*) containing 0.2 mg L⁻¹ 2-chloro-L-phenylalanine as internal standard. Subsequently, the mixture was vortexed vigorously and ultrasonicated for 30 min in ice, then centrifuged at 4 °C 12,000 rpm for 15 min. The supernatant was analyzed by UPLC-ESI-MS/MS (Thermo Fisher, Germering, Germany). The detailed condition of UPLC-ESI-MS/MS and data analysis is shown in Text S3. The metabolic data processing is demonstrated in Text S4.

2.8. Statistical Analysis

All data were analyzed using SPSS (IBM SPSS Statistics 25) [40] by one-way ANOVA with LSD and T-test. The threshold of significant difference of results was at $p < 0.05$ between controls and treatments. The data were reported as the mean and standard deviation ($n = 6$). Different letters represent significance of $p < 0.05$ and asterisk quantity represent significance as the following: "*" for $0.01 < p < 0.05$, "***" for $0.001 < p < 0.01$ and "****" for $p < 0.001$.

3. Results and Discussion

3.1. Fe₇(PO₄)₆ NMs Characterization

The TEM image (Figure 1a) showed that the shape of Fe₇(PO₄)₆ NMs was rod-like and 60 nm in width. EDS spectra (Figure 1b) demonstrated that the NMs were composed of Fe, P, and O. XRD patterns (Figure 1c) exhibited the characteristic peaks of the NMs consistent with the peaks annotated on the standard Fe₇(PO₄)₆ card (PDF Card No. 72-2446). The XPS

results (Figure 1d) displayed two prominent peaks at 712.5 eV and 725.9 eV, corresponding to Fe 2p_{3/2} and Fe 2p_{1/2}, respectively. Fe³⁺ and Fe²⁺ formed Fe 2p_{3/2} peaks at 712.06 eV and 717.24 eV, respectively. Fe 2p_{1/2} also had peaks at 725.35 eV (Fe²⁺) and 730.45 eV (Fe³⁺). The Fe²⁺ in Fe₇(PO₄)₆ NMs might be caused by the partial reduction of Fe³⁺ in FePO₄ because of the presence of carbon from PVP K-30 [41]. The hydrodynamic diameter and Zeta potential of the NMs were 716.89 ± 60.32 nm and −14.37 ± 1.09 mV displayed as Table S3.

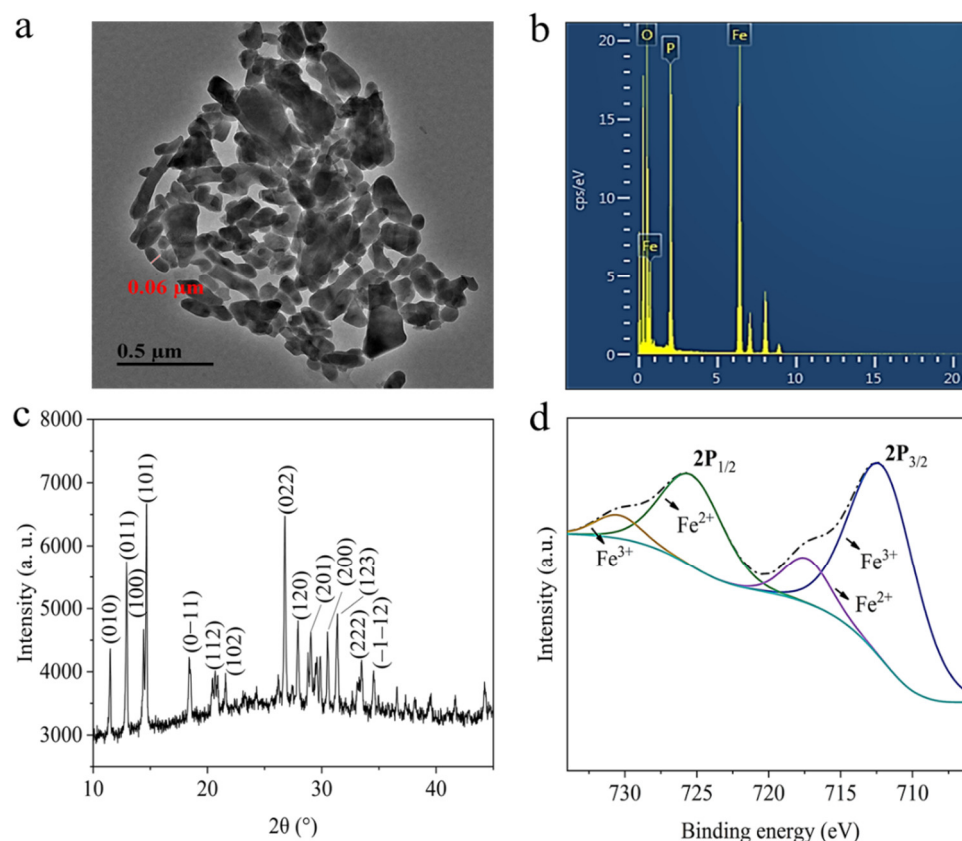


Figure 1. Characterizations of synthesized Fe₇(PO₄)₆ NMs. (a) TEM image; (b) EDS image of Fe, P, and O elements; (c) XRD pattern; (d) XPS diagram.

3.2. Fe₇(PO₄)₆ NMs Enhanced the Flavonoids Accumulation in Tomato Fruits and Related Gene Expressions

After 115 days' growth, the amendment of Fe₇(PO₄)₆ NMs with 5 and 50 mg kg^{−1} had no significant effect on the total fruit weight of tomatoes (Figure 2a,b). However, the flavonoid content in tomato fruits was significantly enhanced by the amendment of Fe₇(PO₄)₆ NMs with 5 and 50 mg kg^{−1} (Figure 2c–e). It was reported that naringenin, quercetin and rutin were three kinds of main flavonoids in tomato fruits [42]. Besides, quercetin and rutin belong to flavonol (a subclass of flavonoids) and the latter is a vital downstream metabolite of the former [42,43]. More importantly, flavonol contains a hydroxyl group at the C3 position, which makes flavonols excellent antioxidants in tomatoes [43]. The content of naringenin was significantly enhanced by 58.54% and 681.39% after the amendment of 5 mg kg^{−1} and 50 mg kg^{−1} Fe₇(PO₄)₆ NMs as compared with control, respectively (Figure 2c). The content of quercetin and rutin in tomato fruits was increased by 33.07 and 80.20% upon 5 mg kg^{−1} Fe₇(PO₄)₆ NMs exposure, and increased by 54.59 and 120.36% upon 50 mg kg^{−1} Fe₇(PO₄)₆ NMs exposure as compared with control, respectively (Figure 2d,e).

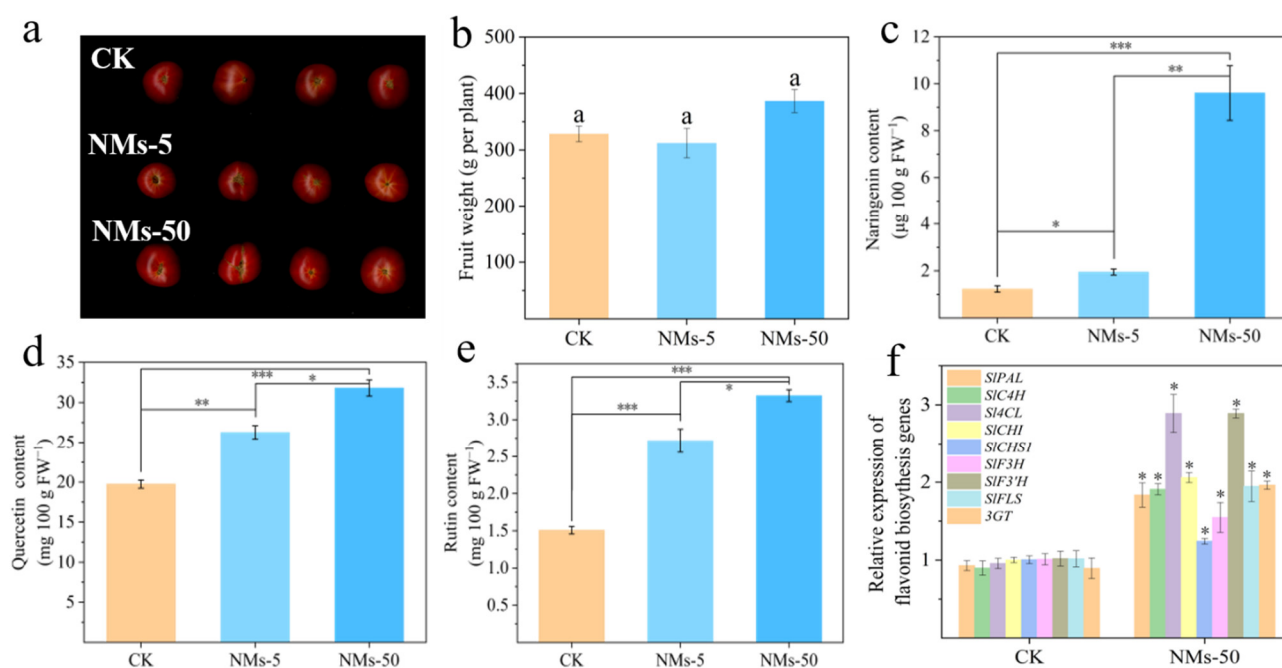


Figure 2. (a) Tomato fruits upon 5 and 50 mg kg^{−1} Fe₇(PO₄)₆ NMs; (b) total fruit yield; (c–e) content of naringenin (c), quercetin (d) and rutin (e) in red mature fruits; (f), relative expression of flavonoids synthesis genes in tomato fruits. Letters of “a” in (b) represent no significance between treatments. Asterisk quantity represents significance as following: “*” for 0.01 < *p* < 0.05, “**” for 0.001 < *p* < 0.01 and “***” for *p* < 0.001.

Flavonoids are derived from the L-phenylalanine via the general phenylpropanoid pathway [44]. The naringin is produced from L-phenylalanine by a series of enzyme catalyzation, which are encoded by *SIPAL*, *SIC4H*, *SI4CL*, *SICH1*, and *SICH51* [44]. The relative expression of *SIPAL*, *SIC4H*, *SI4CL*, *SICH1*, and *SICH51* was significantly upregulated by 83.54, 90.83, 189.09, 24.16 and 105.92% after amendment with Fe₇(PO₄)₆ NMs, respectively (Figure 2f). Meanwhile, *SIF3H*, *SIF3'H*, *SIFLS*, and *SI3GT*, which encode the enzyme catalyzing naringenin to quercetin and rutin [45–47], were significantly upregulated by 54.76, 189.07, 94.73, and 96.15% in Fe₇(PO₄)₆ NMs treatment as compared with control, respectively (Figure 2f). Flavonoids in plants is highly regulated by sucrose, which can act as a signaling molecule to alter genes expression in the flavonoids biosynthetic pathway [12]. Moreover, sucrose in tomato fruits mainly comes from photosynthetic system which requires the participation of various elements. PM H⁺-ATPase pumps proton out of cell to achieve acidification and facilitate the transport of various nutrients. The possible mechanism of flavonoids accumulation in the present study related to PM H⁺-ATPase activity, nutrient uptake, photosynthesis, and sucrose accumulation will be discussed in the following sections.

3.3. Fe₇(PO₄)₆ NMs Improved the Growth of Tomato Seedlings

Visible growth promotion was observed in tomato seedlings upon Fe₇(PO₄)₆ NMs exposure based on the phenotypic images (Figure 3a). As compared with equivalent Fe mass Fe-EDTA treatment and control, 50 mg kg^{−1} Fe₇(PO₄)₆ NMs significantly enhanced tomato root fresh weight by 25.97 and 83.02%, respectively (Figure S1). Tomato shoot fresh weight was also enhanced by 16.67 and 47.78% in 50 mg kg^{−1} Fe₇(PO₄)₆ NMs treatment as compared with equivalent Fe mass Fe-EDTA treatment and control, respectively (Figure S1). The amendment with 50 mg kg^{−1} Fe₇(PO₄)₆ NMs significantly enhanced the root tip numbers by 262.83 and 215.84% as compared with Fe-EDTA and control (Figure 3b). The length, surface area, and volume of roots also showed a significant increase upon Fe₇(PO₄)₆ NM application (Figure S2). The relative content of chlorophyll (SPAD) in tomato

leaves was significantly increased by 7.39 and 36.32% upon $\text{Fe}_7(\text{PO}_4)_6$ NMs amendment as compared with Fe-EDTA and control, respectively (Figure S3a). At the same time, $\text{Fe}_7(\text{PO}_4)_6$ NMs elevated Pn by 14.81 and 31.45% over Fe-EDTA and Control (Figure 3c). Gs, Ci, and E were also more improved by 19.30, 0.74 and 4.45% than Fe-EDTA, and by 39.05, 3.79 and 19.69% than control, respectively (Figure S3b–d). The increase of SPAD value and photosynthetic parameters fully indicated that the application of $\text{Fe}_7(\text{PO}_4)_6$ NMs significantly improved the photosynthesis and growth potential of tomato seedlings. It is reported that Fe-based NMs amendment could enhance the nutrient element uptake, and then promote the photosynthesis and growth of plants, as Fe is a crucial element for photosynthesis [48,49]. Therefore, the content of nutrient element in tomato shoots and roots was analyzed.

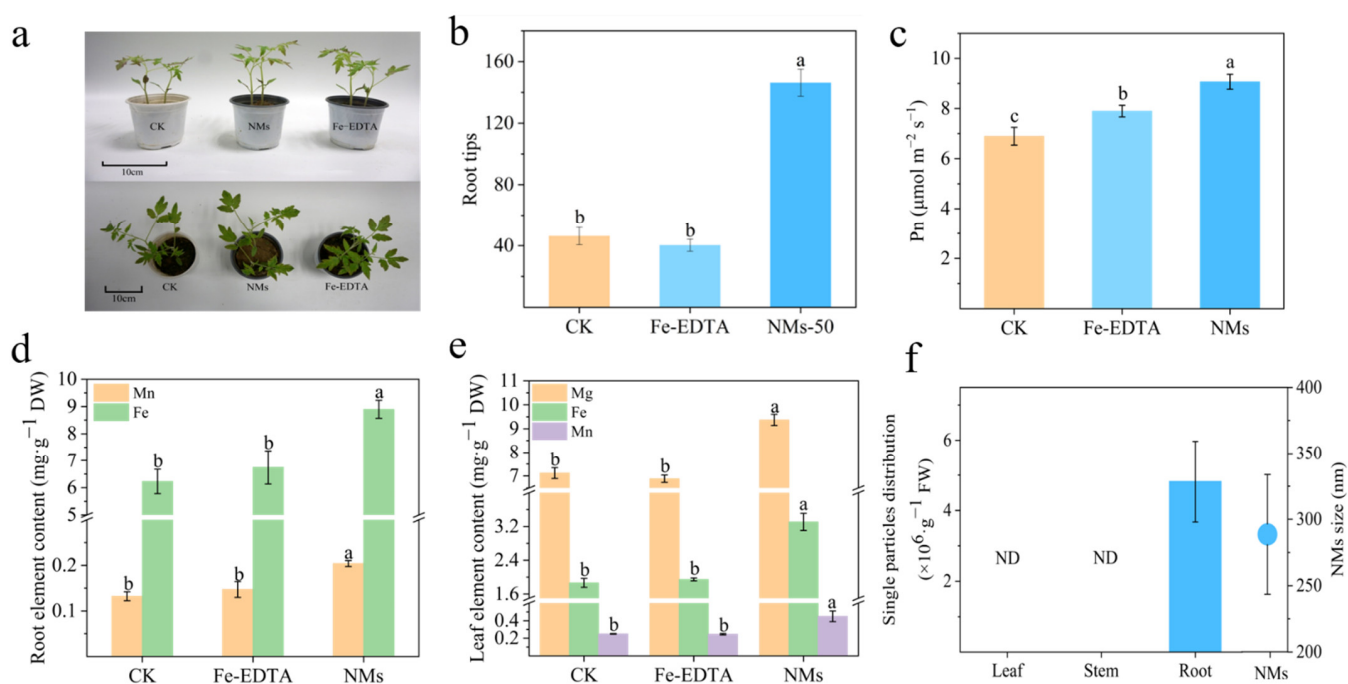


Figure 3. The impacts of $\text{Fe}_7(\text{PO}_4)_6$ NMs on tomato seedling growth. (a) tomato phenotype; (b) root tips number; (c) Pn of the fourth fully unfolded true leaf; (d,e) element content of significant increased by NMs treatment in roots and shoots; (f) single particles distribution in leaf, stem and root of $\text{Fe}_7(\text{PO}_4)_6$ NMs and average size of NMs. Different letters in (b–e) represent significance of $p < 0.05$. ND in (f) means not detected.

In roots, Mn content in NMs treatment was markedly more accumulated by 38.75% than Fe-EDTA and 54.11% than control (Figure 3d). Fe content in $\text{Fe}_7(\text{PO}_4)_6$ NMs was increased by 31.85 and 42.86% over Fe-EDTA and control, respectively (Figure 3d). In shoots, Fe content greatly increased by 69.74 and 77.01% over Fe-EDTA and control. Mn content significantly rose by 82.89 and 80.26% over Fe-EDTA and control. In addition, Mg accumulated significantly by 35.99 and 31.60% over Fe-EDTA and control, respectively (Figure 3e). Fe contributes to electron transfer process, and is essential for cytochrome P450 [50]. Mn is a key element for oxygen evolution required in OEC (oxygen evolving complex) existed in PSII (Photosystem II) [51]. Mg acts as cofactor of a series of enzymes involved in photosynthesis carbon sequestration and metabolism [52]. The increase of Fe, Mn and Mg surely strengthened photosynthesis. In addition, during the flavonoid synthesis, Fe was vital for 2-ODD oxygenases in flavonoid synthase [26]. The obvious accumulation of Fe in tomato leaves can also elevate flavonoids synthesis potential. The enhanced Fe content in tomato seedlings could be attributed to (1) $\text{Fe}_7(\text{PO}_4)_6$ NMs as an efficient Fe source, which enhanced the bioavailable Fe content in soils. It was reported that FePO_4 NMs applied in soil could act as an efficient source of Fe and P as compared to

bulk FePO_4 due to its sub-micron size, which make it easier to reach the root surface and rapidly dissolved [53]. Our results of SP-ICP-MS demonstrated that Fe-bearing particles (average 288.62 nm) were detected in roots upon $\text{Fe}_7(\text{PO}_4)_6$ NMs exposure (Figure 3f) and might explain how $\text{Fe}_7(\text{PO}_4)_6$ NMs entered the roots and enhanced bioavailable Fe in tomatoes; (2) $\text{Fe}_7(\text{PO}_4)_6$ NMs activated the response of tomato to acidify the rhizosphere soils, subsequently enhancing the bioavailability of Fe.

3.4. $\text{Fe}_7(\text{PO}_4)_6$ NMs Promoted PM H^+ ATPase and IAA Content in Root

Based on NMT results, H^+ in the root elongation region showed extremely significant outflow, at $5.87 \text{ pmol}\cdot\text{cm}^{-2}\cdot\text{s}^{-1}$ after the application with $\text{Fe}_7(\text{PO}_4)_6$ NMs (Figure 4a). With the treatment of Fe-EDTA, roots showed little net H^+ efflux ($0.37 \text{ pmol}\cdot\text{cm}^{-2}\cdot\text{s}^{-1}$) which meant effect of rhizosphere acidification was weaker compared to control ($-0.60 \text{ pmol}\cdot\text{cm}^{-2}\cdot\text{s}^{-1}$) (Figure 4a). The relative expressions of *LHA* in roots were examined and results showed that *LHA2* and *LHA4* were significantly upregulated with Fe-EDTA by 1.74 and 4.44 folds compared to control, respectively, when no significance of *LHA1* was observed (Figure 4b). NMs significantly upregulated *LHA1*, *LHA2* and *LHA4* by 3.28, 1.30 and 8.94 folds over control, respectively (Figure 4b). IAA plays a crucial role in activating plasma membrane (PM) H^+ -ATPase [54]. The concentration of IAA in Fe-EDTA was increased by 66.67% but with no significance over control. $\text{Fe}_7(\text{PO}_4)_6$ NMs treatment significantly increased IAA content by 70.75 and 164.21% as compared to Fe-EDTA and control, respectively (Figure 4c). The above results indicated that NMs induced more IAA accumulation and significantly activated more PM H^+ -ATPases to pump more proton and acidify rhizosphere to obtain nutrient (Figure 4) [55]. The ensuing decrease of apoplastic pH would alter the activity of modification proteins, e.g., pectin methylesterases, xyloglucan endotransglycosylase/hydrolases, and expansins, leading to the changes in extensibility of root cell wall. These results illustrated that the tomato roots were stimulated to pump large number of protons to acidify the rhizosphere by $\text{Fe}_7(\text{PO}_4)_6$ NMs. A few researches mentioned that NMs activated PM H^+ ATPase in roots and pump out protons into apoplast and acidify their rhizosphere, finally increased NH_4^+ , P, K, Fe availability in soil [23,24]. According to acid growth theory [56], the decrease of apoplast pH activates cell wall-loosening enzymes, which could make cell expand along with turgor pressure and increase root elongation. H^+ flux and PM H^+ ATPase activity also has critical influence on elements uptake of roots. Plants have a strategy that releases protons into the rhizosphere by PM H^+ ATPase, reducing the pH of the rhizosphere to induce elements dissolution, thus increasing the absorption of nutrients [20]. Moreover, elevated PM H^+ -ATPase activity could hyperpolarize the PM, increasing the energy for nutrient uptake, which is necessary to maintain water uptake and thus the turgor pressure that forces cell wall expansion.

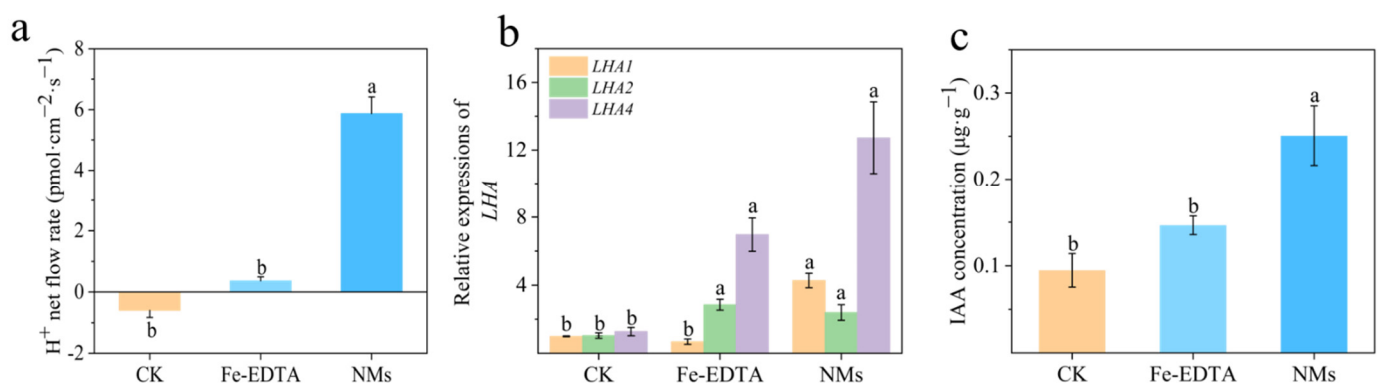


Figure 4. $\text{Fe}_7(\text{PO}_4)_6$ NMs stimulated root PM H^+ ATPase and IAA accumulation. (a) H^+ net flow rate of tomato seedling root elongation zone. Negative value means H^+ influx and positive value means efflux. (b) relative expressions of *LHA* in tomato roots. (c) IAA concentration in tomato roots. Different letters in represent significance of $p < 0.05$.

3.5. $Fe_7(PO_4)_6$ NMs Up-Regulated Sucrose Transporter and Sucrose Accumulation in Fruits

Sucrose is the product of photosynthesis in leaves and is transferred to other tissues by SUT (sucrose transporter) [57]. To further investigate the in planta sucrose transport, gene expressions of sucrose transporter in leaves of fourth leaf stage were analyzed. The qRT-PCR results demonstrated that *SISUT1*, *SISUT2*, and *SISUT4* in plants exposed to $Fe_7(PO_4)_6$ NMs were upregulated significantly over control and Fe-EDTA (Figure 5a). The up-regulation of *SISUT* in leaves indicated sucrose was transported from leaves to flowers more efficiently; tomato fruit setting and fruit sucrose accumulation would be thus increased [19]. Accordingly, sucrose concentration in tomato fruits by $Fe_7(PO_4)_6$ NMs was significantly increased by 21.15% as compared with control (Figure 5b). Sucrose upregulates flavonoid biosynthetic genes and induces expression of transcription factors to promote flavonoid synthesis in fruits [14]. It was reported that sucrose acted as an endogenous inducer in upregulating the expression of anthocyanin biosynthetic and regulatory genes of *MrMYB1* [58]. Sucrose would also increase transcript levels of early anthocyanin biosynthesis genes including *CHI*, *CHS*, and *C4H* in *Arabidopsis* [59,60]. Also, sucrose could be metabolized into glucose and the latter acted as the substrate of pentose phosphate pathway for providing flavonoid synthesis precursors [11]. As sucrose accumulation increased in NM treatment, it could act as a signal to upregulate significantly flavonoid synthesis genes and might provide more precursors in tomato fruits compared to control.

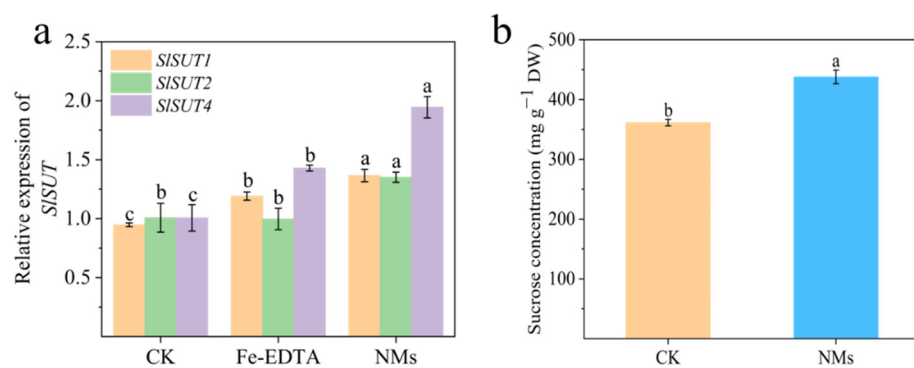


Figure 5. Relative expressions of sucrose transporter genes (a) and sucrose content in tomato fruits (b) Different letters in represent significance of $p < 0.05$.

3.6. Mechanisms of Enhanced Flavonoids Accumulation in Tomato Fruits by Integration Analysis of Transcriptomics and Metabolomics

3.6.1. Transcriptomic Analysis of Tomato Fruits by $Fe_7(PO_4)_6$ NMs

To explore the molecular mechanism underlying the enhanced flavonoid synthesis by $Fe_7(PO_4)_6$ NMs, transcriptomic analysis of tomato fruits was performed. PCA (principal component analysis) plot showed that CK and $Fe_7(PO_4)_6$ NMs treatment were clearly separated along PC1 (92% of total variance) (Figure 6a). The differentially expressed genes (DEGs) were annotated and used for GO (Figures 6b and 7a) and KEGG (Figures 6c and 7b) enrichment analysis. For the functional classification in GO database, DEGs annotated with “cellular process”, “metabolic process”, “biological process” and “response to stimulus” were most abundant within the biological process category (Figure S4). In molecular function, DEGs were enriched in “catalytic activity” and “binding”. As for cellular component, DEGs were enriched in “cell part”, “organelle” and “membrane”. “metabolic process”, “response to stimulus” and “catalytic activity” were related with flavonoid synthesis [61,62], and secondary metabolic process, phenylpropanoid metabolic process, and secondary metabolite biosynthetic process were significantly altered upon $Fe_7(PO_4)_6$ NMs relative to CK. In order to further understand the DEG functions, the KEGG pathway enrichment was performed. Among analysis results, pathways related to flavonoid synthesis like phenylpropanoid biosynthesis (ko00940), biosynthesis of secondary metabolites (ko01110) and

phenylalanine metabolism (ko00360) were significantly enriched in tomato fruits (Figures 6c and 7b).

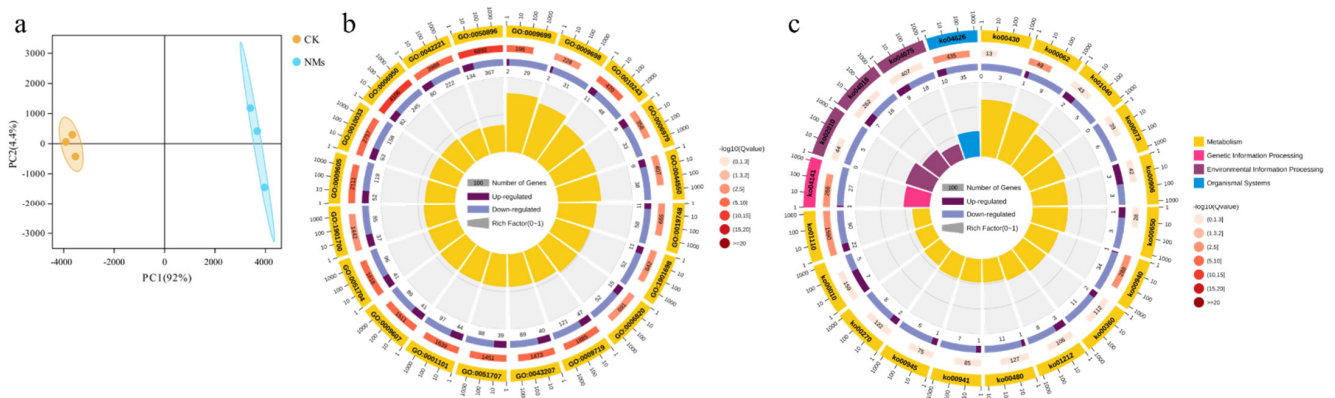


Figure 6. Transcriptomic profiling in tomato fruits upon $\text{Fe}_7(\text{PO}_4)_6$ NM exposure. (a), PCA plot; (b), classification of DEGs in GO; (c), KEGG enrichment analysis of DEGs.

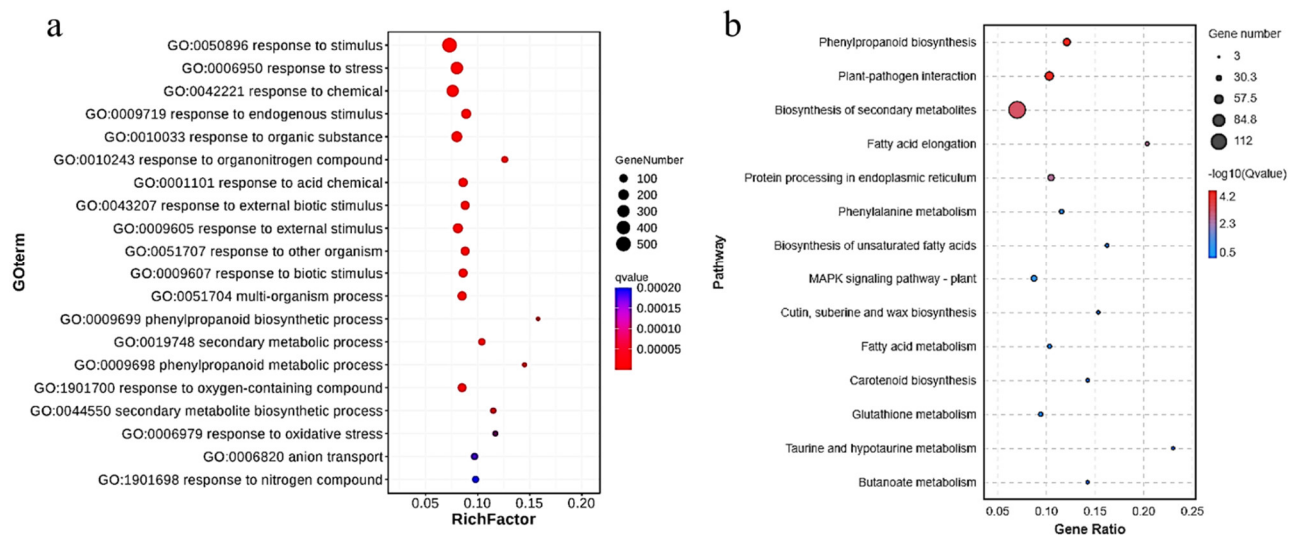


Figure 7. GO and KEGG enrichment of DEGs in tomato fruits upon $\text{Fe}_7(\text{PO}_4)_6$ NMs exposure. (a) GO enrichment; (b) KEGG enrichment of pathways.

Specifically, there were 11 DEGs of tomato fruits involved in flavonoid synthesis (Table S4). The transcriptional level of *SISS*, *SITPS6*, *SITPS11* and *SITKL-1*, belonging to sucrose metabolism pathway [63–65], was significantly upregulated by 101.43, 131.24, 118.71 and 32.17% over CK, indicating that $\text{Fe}_7(\text{PO}_4)_6$ NMs elevated transcriptional regulation of sucrose metabolism pathway. In shikimic acid pathway, only *SIDHQ-SOR* was detected, and was significantly downregulated by 15.20%; thus, shikimic acid pathway was suppressed by $\text{Fe}_7(\text{PO}_4)_6$ NMs. Li et al. [66], found that most of the shikimate pathway genes showed a decreased transcript abundance in strawberry fruits injected with 100 μL of ABA (1 μM). Our transcriptomic results showed that *PYL*, the gene encoding ABA receptor, was significantly upregulated (188.46%) with $\text{Fe}_7(\text{PO}_4)_6$ NMs treatment. High expression of *PYL* represented ABA receptor was activated, indicating that ABA content was increased [67,68]. In phenylalanine pathway, transcriptional level of *SIEPSPS-1* (encoding the enzyme catalyzes the formation of EPSP (5-enolpyruvyl shikimate-3-phosphate) from shikimate-3-phosphate and phosphoenolpyruvate) [69] and *SICM2* (encoding the enzyme rearranges the enolpyruvyl side chain of chorismate to form prephenate) [70] were significantly downregulated by 15.63% and 34.99% (Table S4). In final flavonoid

biosynthesis, the transcriptional level of *Sl4CL* and *SlCHI* was significantly increased by 20.75 and 123.53%. In tomato fruits, *SIMYB12* was examined as the TF correlated well with the expression of flavonoid synthesis genes [71–73]. *SIMYB12* can lead to the flavonoid accumulation and strongly regulate flavonoid synthesis genes [73], and was upregulated significantly by $\text{Fe}_7(\text{PO}_4)_6$ NMs (Table S4). Overall, the expression pattern of genes in fruits upon $\text{Fe}_7(\text{PO}_4)_6$ NMs showed a preference for final flavonoid biosynthesis activation.

3.6.2. Metabolic Analysis of Tomato Fruits Exposed to $\text{Fe}_7(\text{PO}_4)_6$ NMs

The impact of $\text{Fe}_7(\text{PO}_4)_6$ NMs on metabolic profiles of tomato fruits was further investigated; the PCA score plot (Figure S5a) indicated that metabolic levels were significantly different between CK and $\text{Fe}_7(\text{PO}_4)_6$ NMs (66.3% of total variance). In all samples, 217 metabolites were identified and annotated and 50 relative quantitation of differentially expressed metabolites (DEMs) were selected according to the standard of VIP (variable importance in projection) > 1 and $p < 0.05$ and illustrated (Figure S5b, Table S5). In sucrose metabolism pathway, UDP-glucose (the production of sucrose catalyzed by sucrose synthase), trehalose and D-Glucose-6P (G6P) were detected and increased to 17.50, 28.38 and 10.13% compared with control, respectively (Table S6), and it was because the transcriptional levels of *SISS*, *SITPS6* and *SITPS11*, regulating enzymes catalyzing sucrose to trehalose, were significantly upregulated (Table S4) [74,75]. However, the metabolites of shikimic acid pathway and phenylalanine synthesis pathway were not detected.

In this study, 11 DEGs and 6 DEMs were identified in the process of sucrose metabolism to the final flavonoid biosynthesis of tomato fruits. Three transcriptional genes (*SISS*, *SITPS6* and *SITPP*) of enzymes catalyzing sucrose to trehalose were significantly upregulated by $\text{Fe}_7(\text{PO}_4)_6$ NMs in tomato fruits (Figure 8a) [63–65]. The significant increase of UDP-glucose (product of sucrose degradation regulated by *SISS*) markedly elevated the content of trehalose (product of the catalytic processes regulated by *SITPS6* and *SITPP*). These up-regulations of DEGs and DEMs could jointly promote the significant increase of G6P (Table S6), which is a key common precursor of glycolysis and pentose phosphate process, and its final products PEP and erythrose-4-phosphate (E4P) serve as raw materials for shikimic acid pathway [76]. In addition, although no DEG was detected in the pentose phosphate pathway, *SITKL-1*, which regulates the production of E4P derived from G6P in glycolysis, was significantly increased. Therefore, $\text{Fe}_7(\text{PO}_4)_6$ NMs significantly increased the transcriptional regulation level of sucrose metabolism in tomato fruits and accelerated sucrose conversion, providing more adequate materials for downstream pathways.

Surprisingly, *SIDHQ-SOR* detected in the shikimic acid pathway was significantly down-regulated (Figure 8b). Increased ABA significantly down-regulated the shikimic acid pathway related genes during strawberry ripening [66]. We investigated the transcription level of ABA signaling pathway and found that *SIPYL4*, the regulation gene of ABA receptor PYL was significantly elevated, suggesting that ABA response pathway was activated in tomato fruits and inhibited the expression of *SIDHQ-SOR* in shikimic acid pathway [68]. ABA was obviously increased by NMs (Figure S6). Some studies demonstrated that ABA acts as a crucial signal to promote flavonoids [77,78]. In short, ABA enhances flavonoid synthesis, though shikimate pathway is suppressed. Thus, it could explain the reason why shikimate pathway is not consistent with increased flavonoid synthesis but regulated by endogenous ABA. The transcription level was also down-regulated in the phenylalanine synthesis pathway following shikimic acid pathway (Figure 8c), which may be caused by the decrease of substances flowing into phenylalanine synthesis pathway due to the decreased transcription level of a shikimic acid pathway.

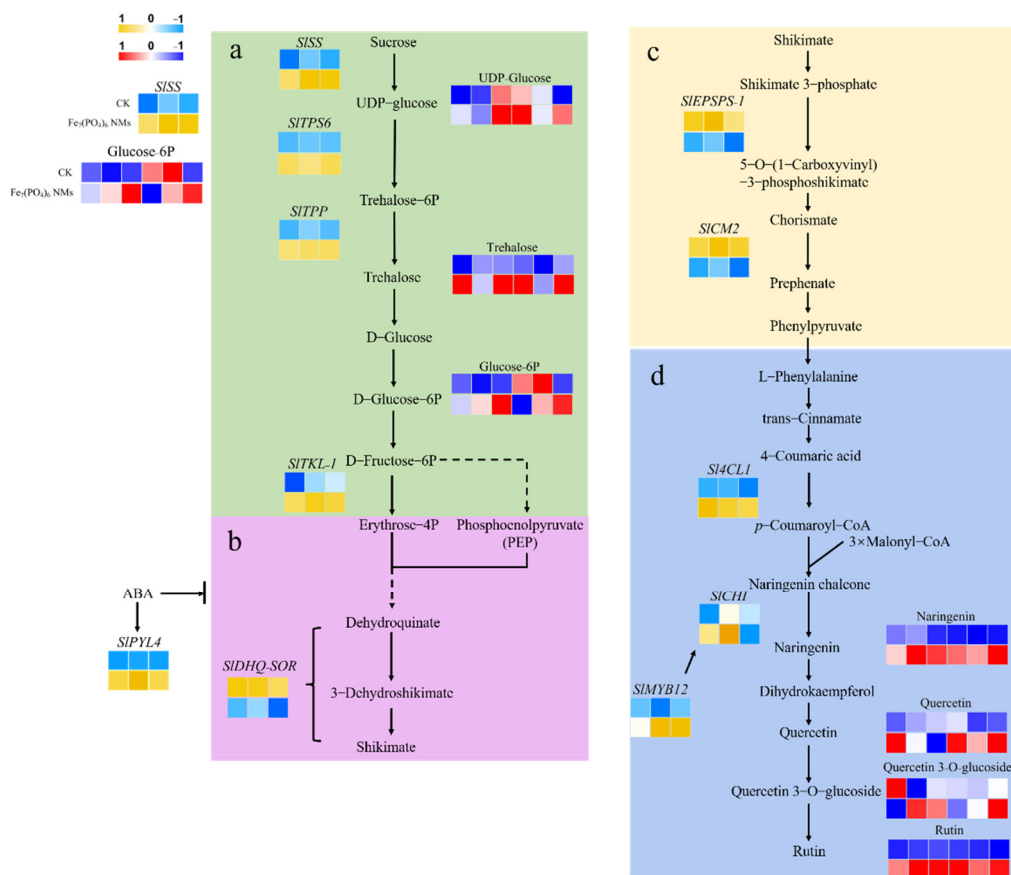


Figure 8. Transcriptomic and metabolomic pathways of flavonoids synthesis enhanced by $\text{Fe}_7(\text{PO}_4)_6$ NMs in tomato fruits. (a) sucrose metabolism; (b) shikimic acid pathway; (c) phenylalanine synthesis pathway; (d) flavonoid biosynthesis pathway. The data of transcriptomics and metabolomics were normalized before comparison in heatmaps. The color scheme represents decrease or increase of value of $\log_2(\text{fold change})$ and the fold change indicated the FPKM ratio of DEG and response value ratio of DEM in 50 mg kg^{-1} NMs to control. At transcriptional level, blue represents downregulation and yellow means upregulation; at metabolic level, blue represents downregulation and red means upregulation. Upper squares represent samples of CK and lower ones represent samples of NMs.

In the final flavonoid biosynthesis pathway, two DEGs of *SI4CL1* and *SICH1* were significantly increased (Figure 8d). *SI4CL1* catalyzes 4-coumaric acid to *p*-coumaroyl-CoA, providing the precursor for the synthesis of naringenin chalcone. The transformation from naringenin chalcone to naringenin was catalyzed by *SICH1*, and *SICH1* was found to be the rate-limiting enzyme of flavonoid synthesis [79]. In our study, the upregulated *SICH1* indicated that flavonoid biosynthesis was significantly accelerated. Most other types of flavonoids are modified based on naringenin [80]. The significantly increased content of naringenin (Figure 2c) illustrated enhanced downstream flavonoid level. Quercetin and rutin are the catalyzed products of naringenin in flavonol synthesis pathway. As the important antioxidant substances in tomato [81], the metabolic levels of these two flavonols were also significantly increased (Figure 2c), indicating that the antioxidant ability of tomato was significantly improved. Flavonoid synthesis is closely regulated by TFs such as *SIMYB12*, which was improved as an extensive positive role in flavonoid biosynthesis pathways of tomatoes [72,73]. The markedly upregulated transcriptional level of *SIMYB12* implied that flavonoid synthesis at the level of transcriptional regulation was enhanced by $\text{Fe}_7(\text{PO}_4)_6$ NMs. Hence, $\text{Fe}_7(\text{PO}_4)_6$ NMs promoted flavonoid synthesis by enhancing the transcription level and ultimately induced flavonoid accumulation in tomato fruits.

4. Conclusions

After treated with 50 mg kg⁻¹ Fe₇(PO₄)₆ NMs, the content of IAA in tomato seedlings roots was significantly increased, and the activity of PM H⁺ ATPase was enhanced over control and equivalent Fe mass Fe-EDTA fertilizer, leading to root development and rhizosphere acidification. The uptake of nutrient elements was elevated, subsequently enhancing the photosynthesis. The sucrose transporter genes of *SISUT1*, *SISUT2*, and *SISUT4* were also markedly upregulated by Fe₇(PO₄)₆ NMs, and more sucrose was transported from leaves to flowers to promote fruit setting and yield potential. Compared with the control, the accumulation of sucrose in fruit treated by Fe₇(PO₄)₆ NMs indirectly led to the increase of flavonoid synthesis precursors. Transcriptome and metabolome data demonstrated the positive activation of a sucrose metabolism pathway and an ultimate flavonoid biosynthesis pathway in tomato fruits by Fe₇(PO₄)₆ NMs, and qRT-PCR results verified the up-regulation of flavonoid synthesis genes. Our findings reveal the potential of NMs application to promote the quality of fruits with flavonoids, which is useful for the development of high-quality nano-enabled agriculture in the future.

Supplementary Materials: The following supporting information can be downloaded at: <https://www.mdpi.com/article/10.3390/nano12081341/s1>. Figure S1: Biomass of roots and shoots in different treatments. Different letters above columns (a, b and c) represent significance of $p < 0.05$ and there is no significant difference between “ab” and “a”, nor between “ab” and “b”; Figure S2: Root length (a), surface area (b), volume (c), and average diameter (d) of tomato seedlings exposed to Fe₇(PO₄)₆ NMs. Different letters above columns (a, b and c) represent significance of $p < 0.05$; Figure S3: Photosynthetic parameters of tomato seedlings. a, chlorophyll SPAD value; b-d, Gs, Ci, and E value. Different letters above columns (a, b and c) represent significance of $p < 0.05$; Figure S4: GO enrichment analysis of DEGs (a) and KEGG enrichment analysis (b) in tomato fruits; Figure S5: PCA plot (a) and DEMs heatmap (b) in tomato fruits. VIP value > 1 and $p < 0.05$ were set as DEMs standard. Figure S6: ABA content in fruits. Different letters above columns (a and b) represent significance of $p < 0.05$. Table S1. The properties of soil used in this research; Table S2. Primer sequences of flavonoids synthesis genes, PM H⁺ ATPase genes and sucrose transporter genes; Table S3. Hydrodynamic diameter and zeta potential of Fe₇(PO₄)₆ NMs; Table S4. Fpkms value of DEGs in pathways from sucrose metabolism to flavonoid synthesis pathway; Table S5. Differentially expressed metabolites (DEMs) selected of tomato fruits in CK and upon Fe₇(PO₄)₆ NMs exposure by VIP > 1 and $p < 0.05$. Name of metabolites and its codes were corresponding to heatmap (Figure S5b); Table S6. Relative content of metabolites detected in sucrose metabolism pathway; References [82–86] are cited in the supplementary materials.

Author Contributions: Conceptualization, Z.W. and L.Y.; methodology, X.L.; software, X.L.; validation, X.L., L.Y. and X.C.; formal analysis, C.W.; investigation, F.C.; resources, J.W.; data curation, Y.F.; writing—original draft preparation, Z.W. and X.L.; writing—review and editing, L.Y. and B.X.; visualization, Y.F.; supervision, L.Y.; project administration, F.C.; funding acquisition, Z.W. and L.Y. All authors have read and agreed to the published version of the manuscript.

Funding: This research was supported by the National Natural Science Foundation of China (41820104009, 41807378, 42007299, and 42077296) and Special Grade of the Financial Support from the China Postdoctoral Science Foundation (2021T140278).

Institutional Review Board Statement: Not applicable.

Informed Consent Statement: Not applicable.

Data Availability Statement: RNA-Seq data generated from *Solanum lycopersicum* L. has been submitted to the NCBI under project number PRJNA824998 (<https://www.ncbi.nlm.nih.gov/sra/PRJNA824998>, access date: 11 April 2022). The data presented in this study are available on request from the corresponding author.

Conflicts of Interest: The authors declare no conflict of interest.

References

1. Wen, L.; Zhou, T.; Jiang, Y.; Chang, S.K.; Yang, B. Prenylated Flavonoids in Foods and Their Applications on Cancer Prevention. *Crit. Rev. Food Sci. Nutr.* **2021**, *62*, 1–14. [[CrossRef](#)] [[PubMed](#)]
2. He, D.; Ru, X.; Wen, L.; Wen, Y.; Jiang, H.; Bruce, I.C.; Jin, J.; Ma, X.; Xia, Q. Total Flavonoids of *Flos Chrysanthemi* Protect Arterial Endothelial Cells Against Oxidative Stress. *J. Ethnopharmacol.* **2012**, *139*, 68–73. [[CrossRef](#)] [[PubMed](#)]
3. Srivastava, S.; Somasagara, R.R.; Hegde, M.; Nishana, M.; Tadi, S.K.; Srivastava, M.; Choudhary, B.; Raghavan, S.C. Quercetin, a Natural Flavonoid Interacts with DNA, Arrests Cell Cycle and Causes Tumor Regression by Activating Mitochondrial Pathway of Apoptosis. *Sci. Rep.* **2016**, *6*, 24049. [[CrossRef](#)] [[PubMed](#)]
4. Varshney, R.; Mishra, R.; Das, N.; Sircar, D.; Roy, P. A Comparative Analysis of Various Flavonoids in the Regulation of Obesity and Diabetes: An in vitro and in vivo Study. *J. Funct. Foods* **2019**, *59*, 194–205. [[CrossRef](#)]
5. Perez-Cano, F.J.; Castell, M. Flavonoids, Inflammation and Immune System. *Nutrients* **2016**, *8*, 659. [[CrossRef](#)]
6. Bondonno, N.P.; Dalgaard, F.; Kyro, C.; Murray, K.; Bondonno, C.P.; Lewis, J.R.; Croft, K.D.; Gislason, G.; Scalbert, A.; Cassidy, A. Flavonoid intake is associated with lower mortality in the Danish Diet Cancer and Health Cohort. *Nat. Commun.* **2019**, *10*, 3651. [[CrossRef](#)]
7. Willits, M.G.; Kramer, C.M.; Prata, R.T.N.; De Luca, V.; Potter, B.G.; Steffens, J.C.; Graser, G. Utilization of the genetic resources of wild species to create a nontransgenic high flavonoid tomato. *J. Agric. Food Chem.* **2005**, *53*, 1231–1236. [[CrossRef](#)]
8. Stewart, A.J.; Bozonnet, S.; Mullen, W.; Jenkins, G.I.; Lean, M.E.J.; Crozier, A. Occurrence of flavonols in tomatoes and tomato-based products. *J. Agric. Food Chem.* **2000**, *48*, 2663–2669. [[CrossRef](#)]
9. Hernandez-Hernandez, H.; Quiterio-Gutierrez, T.; Cadenas-Pliego, G.; Ortega-Ortiz, H.; Hernandez-Fuentes, A.D.; Cabrera de la Fuente, M.; Valdes-Reyna, J.; Juarez-Maldonado, A. Impact of Selenium and Copper Nanoparticles on Yield, Antioxidant System, and Fruit Quality of Tomato Plants. *Plants* **2019**, *8*, 355. [[CrossRef](#)]
10. Gonzalez-Moscoso, M.; Martinez-Villegas, N.V.; Cadenas-Pliego, G.; Benavides-Mendoza, A.; Rivera-Cruz, M.D.C.; Gonzalez-Morales, S.; Juarez-Maldonado, A. Impact of Silicon Nanoparticles on the Antioxidant Compounds of Tomato Fruits Stressed by Arsenic. *Foods* **2019**, *8*, 612. [[CrossRef](#)]
11. Li, D.; Zhang, X.; Xu, Y.; Li, L.; Aghdam, M.S.; Luo, Z. Effect of exogenous sucrose on anthocyanin synthesis in postharvest strawberry fruit. *Food Chem.* **2019**, *289*, 112–120. [[CrossRef](#)] [[PubMed](#)]
12. Lin, S.; Singh, R.K.; Moehninsi, M.; Navarre, D.A. R2R3-MYB transcription factors, *StmiR858* and sucrose mediate potato flavonol biosynthesis. *Hortic. Res.* **2021**, *8*, 25. [[CrossRef](#)] [[PubMed](#)]
13. Jeong, C.Y.; Kim, J.H.; Lee, W.J.; Jin, J.Y.; Kim, J.; Hong, S.W.; Lee, H. *AtMyb56* Regulates Anthocyanin Levels via the Modulation of *AtGPT2* Expression in Response to Sucrose in *Arabidopsis*. *Mol. Cells* **2018**, *41*, 351–361. [[PubMed](#)]
14. Duran-Soria, S.; Pott, D.M.; Osorio, S.; Vallarino, J.G. Sugar Signaling During Fruit Ripening. *Front. Plant Sci.* **2020**, *11*, 564917. [[CrossRef](#)]
15. Payyavula, R.S.; Singh, R.K.; Navarre, D.A. Transcription factors, sucrose, and sucrose metabolic genes interact to regulate potato phenylpropanoid metabolism. *J. Exp. Bot.* **2013**, *64*, 5115–5131. [[CrossRef](#)]
16. Qian, Y.; Zhang, T.; Yu, Y.; Gou, L.; Yang, J.; Xu, J.; Pi, E. Regulatory Mechanisms of *bHLH* Transcription Factors in Plant Adaptive Responses to Various Abiotic Stresses. *Front. Plant Sci.* **2021**, *12*, 677611. [[CrossRef](#)]
17. Cao, Y.; Li, K.; Li, Y.; Zhao, X.; Wang, L. MYB Transcription Factors as Regulators of Secondary Metabolism in Plants. *Biology* **2020**, *9*, 61. [[CrossRef](#)]
18. Zhao, L.; Gao, L.; Wang, H.; Chen, X.; Wang, Y.; Yang, H.; Wei, C.; Wan, X.; Xia, T. The R2R3-MYB, *bHLH*, *WD40*, and related transcription factors in flavonoid biosynthesis. *Funct. Integr. Genom.* **2013**, *13*, 75–98. [[CrossRef](#)]
19. Shen, S.; Ma, S.; Liu, Y.; Liao, S.; Li, J.; Wu, L.; Kartika, D.; Mock, H.P.; Ruan, Y.L. Cell Wall Invertase and Sugar Transporters Are Differentially Activated in Tomato Styles and Ovaries During Pollination and Fertilization. *Front. Plant Sci.* **2019**, *10*, 506. [[CrossRef](#)]
20. Santi, S.; Schmidt, W. Dissecting iron deficiency-induced proton extrusion in *Arabidopsis* roots. *New Phytol.* **2009**, *183*, 1072–1084. [[CrossRef](#)]
21. Haruta, M.; Gray, W.M.; Sussman, M.R. Regulation of the plasma membrane proton pump (H⁺)-ATPase by phosphorylation. *Curr. Opin. Plant Biol.* **2015**, *28*, 68–75. [[CrossRef](#)] [[PubMed](#)]
22. Morth, J.P.; Pedersen, B.P.; Buch-Pedersen, M.J.; Andersen, J.P.; Vilsen, B.; Palmgren, M.G.; Nissen, P. A structural overview of the plasma membrane Na⁺,K⁺-ATPase and H⁺-ATPase ion pumps. *Nat. Rev. Mol. Cell Biol.* **2011**, *12*, 60–70. [[CrossRef](#)] [[PubMed](#)]
23. Kim, J.H.; Oh, Y.; Yoon, H.; Hwang, I.; Chang, Y.S. Iron nanoparticle-induced activation of plasma membrane H⁺-ATPase promotes stomatal opening in *Arabidopsis thaliana*. *Environ. Sci. Technol.* **2015**, *49*, 1113–1119. [[CrossRef](#)] [[PubMed](#)]
24. Zhang, M.; Wang, Y.; Chen, X.; Xu, F.; Ding, M.; Ye, W.; Kawai, Y.; Toda, Y.; Hayashi, Y.; Suzuki, T.; et al. Plasma membrane H⁺-ATPase overexpression increases rice yield via simultaneous enhancement of nutrient uptake and photosynthesis. *Nat. Commun.* **2021**, *12*, 735. [[CrossRef](#)] [[PubMed](#)]
25. Sun, T.; Zhang, J.; Zhang, Q.; Li, X.; Li, M.; Yang, Y.; Zhou, J.; Wei, Q.; Zhou, B. Transcriptome and metabolome analyses revealed the response mechanism of apple to different phosphorus stresses. *Plant Physiol. Biochem.* **2021**, *167*, 639–650. [[CrossRef](#)]
26. Cheng, A.X.; Han, X.J.; Wu, Y.F.; Lou, H.X. The function and catalysis of 2-oxoglutarate-dependent oxygenases involved in plant flavonoid biosynthesis. *Int. J. Mol. Sci.* **2014**, *15*, 1080–1095. [[CrossRef](#)]

27. Yoon, H.; Kang, Y.G.; Chang, Y.S.; Kim, J.H. Effects of Zerovalent Iron Nanoparticles on Photosynthesis and Biochemical Adaptation of Soil-Grown *Arabidopsis thaliana*. *Nanomaterials* **2019**, *9*, 1543. [[CrossRef](#)]
28. Song, H.; Sun, Y.; Jia, X. Hydrothermal synthesis of iron phosphate microspheres constructed by mesoporous polyhedral nanocrystals. *Mater. Charact.* **2015**, *107*, 182–188. [[CrossRef](#)]
29. Wang, Z.; Yue, L.; Dhankher, O.P.; Xing, B. Nano-enabled improvements of growth and nutritional quality in food plants driven by rhizosphere processes. *Environ. Int.* **2020**, *142*, 105831. [[CrossRef](#)]
30. Wang, Z.; Zhu, W.; Chen, F.; Yue, L.; Ding, Y.; Xu, H.; Rasmann, S.; Xiao, Z. Nanosilicon enhances maize resistance against oriental armyworm (*Mythimna separata*) by activating the biosynthesis of chemical defenses. *Sci. Total Environ.* **2021**, *778*, 146378. [[CrossRef](#)]
31. Xu, L.; Wang, Z.; Zhao, J.; Lin, M.; Xing, B. Accumulation of metal-based nanoparticles in marine bivalve mollusks from offshore aquaculture as detected by single particle ICP-MS. *Environ. Pollut.* **2020**, *260*, 114043. [[CrossRef](#)] [[PubMed](#)]
32. Ye, J.Y.; Tian, W.H.; Zhou, M.; Zhu, Q.Y.; Du, W.X.; Zhu, Y.X.; Liu, X.X.; Lin, X.Y.; Zheng, S.J.; Jin, C.W. STOP1 activates NRT1.1-mediated nitrate uptake to create a favorable rhizospheric pH for plant adaptation to acidity. *Plant Cell* **2021**, *33*, 3658–3674. [[CrossRef](#)] [[PubMed](#)]
33. Wei, D.; Zhang, W.; Wang, C.; Meng, Q.; Li, G.; Chen, T.H.H.; Yang, X. Genetic engineering of the biosynthesis of glycinebetaine leads to alleviate salt-induced potassium efflux and enhances salt tolerance in tomato plants. *Plant Sci.* **2017**, *257*, 74–83. [[CrossRef](#)] [[PubMed](#)]
34. Dwivedi, A.D.; Yoon, H.; Singh, J.P.; Chae, K.H.; Rho, S.C.; Hwang, D.S.; Chang, Y.S. Uptake, Distribution, and Transformation of Zerovalent Iron Nanoparticles in the Edible Plant *Cucumis sativus*. *Environ. Sci. Technol.* **2018**, *52*, 10057–10066. [[CrossRef](#)]
35. Xu, W.; Shi, W.; Jia, L.; Liang, J.; Zhang, J. TFT6 and TFT7, two different members of tomato 14-3-3 gene family, play distinct roles in plant adaptation to low phosphorus stress. *Plant Cell Environ.* **2012**, *35*, 1393–1406. [[CrossRef](#)]
36. Xiao, Z.; Jiang, L.; Chen, X.; Zhang, Y.; Defosse, E.; Hu, F.; Liu, M.; Rasmann, S. Earthworms suppress thrips attack on tomato plants by concomitantly modulating soil properties and plant chemistry. *Soil Biol. Biochem.* **2019**, *130*, 23–32. [[CrossRef](#)]
37. Feng, Y.-X.; Yu, X.-Z.; Mo, C.-H.; Lu, C.-J. Regulation Network of Sucrose Metabolism in Response to Trivalent and Hexavalent Chromium in *Oryza sativa*. *J. Agric. Food Chem.* **2019**, *67*, 9738–9748. [[CrossRef](#)]
38. Hu, Y.; Zhang, J.; Kong, W.; Zhao, G.; Yang, M. Mechanisms of antifungal and anti-aflatoxigenic properties of essential oil derived from turmeric (*Curcuma longa* L.) on *Aspergillus flavus*. *Food Chem.* **2017**, *220*, 1–8. [[CrossRef](#)]
39. Garcia, C.J.; Garcia-Villalba, R.; Gil, M.I.; Tomas-Barberan, F.A. LC-MS Untargeted Metabolomics To Explain the Signal Metabolites Inducing Browning in Fresh-Cut Lettuce. *J. Agric. Food Chem.* **2017**, *65*, 4526–4535. [[CrossRef](#)]
40. IBM Corp. *IBM SPSS Statistics for Windows, Version 25.0*; IBM Corp.: Armonk, NY, USA, 2017.
41. Lim, B.; Lu, X.; Jiang, M.; Camargo, P.H.C.; Cho, E.C.; Lee, E.P.; Xia, Y. Facile Synthesis of Highly Faceted Multioctahedral Pt Nanocrystals through Controlled Overgrowth. *Nano Lett.* **2008**, *8*, 4043–4047. [[CrossRef](#)]
42. Slimestad, R.; Verheul, M. Review of flavonoids and other phenolics from fruits of different tomato (*Lycopersicon esculentum* Mill.) cultivars. *J. Sci. Food Agr.* **2009**, *89*, 1255–1270. [[CrossRef](#)]
43. Schijlen, E.; Ric de Vos, C.H.; Jonker, H.; van den Broeck, H.; Molthoff, J.; van Tunen, A.; Martens, S.; Bovy, A. Pathway engineering for healthy phytochemicals leading to the production of novel flavonoids in tomato fruit. *Plant Biotechnol. J.* **2006**, *4*, 433–444. [[CrossRef](#)]
44. Nakayama, T.; Takahashi, S.; Waki, T. Formation of Flavonoid Metabolons: Functional Significance of Protein-Protein Interactions and Impact on Flavonoid Chemodiversity. *Front. Plant Sci.* **2019**, *10*, 821. [[CrossRef](#)] [[PubMed](#)]
45. Tohge, T.; de Souza, L.P.; Fernie, A.R. Current understanding of the pathways of flavonoid biosynthesis in model and crop plants. *J. Exp. Bot.* **2017**, *68*, 4013–4028. [[CrossRef](#)] [[PubMed](#)]
46. Shinozaki, Y.; Nicolas, P.; Fernandez-Pozo, N.; Ma, Q.; Evanich, D.J.; Shi, Y.; Xu, Y.; Zheng, Y.; Snyder, S.I.; Martin, L.B.B.; et al. High-resolution spatiotemporal transcriptome mapping of tomato fruit development and ripening. *Nat. Commun.* **2018**, *9*, 364. [[CrossRef](#)] [[PubMed](#)]
47. Suzuki, T.; Kim, S.-J.; Yamauchi, H.; Takigawa, S.; Honda, Y.; Mukasa, Y. Characterization of a flavonoid 3-O-glucosyltransferase and its activity during cotyledon growth in buckwheat (*Fagopyrum esculentum*). *Plant Sci.* **2005**, *169*, 943–948. [[CrossRef](#)]
48. Shankamma, K.; Yallappa, S.; Shivanna, M.B.; Manjanna, J. Fe₂O₃ magnetic nanoparticles to enhance *S. lycopersicum* (tomato) plant growth and their biomineralization. *Appl. Nanosci.* **2015**, *6*, 983–990. [[CrossRef](#)]
49. Yan, L.; Li, P.; Zhao, X.; Ji, R.; Zhao, L. Physiological and metabolic responses of maize (*Zea mays*) plants to Fe₃O₄ nanoparticles. *Sci. Total Environ.* **2020**, *718*, 137400. [[CrossRef](#)]
50. Nakanishi-Masuno, T.; Shitan, N.; Sugiyama, A.; Takanashi, K.; Inaba, S.; Kaneko, S.; Yazaki, K. The *Crotalaria juncea* metal transporter CjNRAMP1 has a high Fe uptake activity, even in an environment with high Cd contamination. *Int. J. Phytoremediation* **2018**, *20*, 1427–1437. [[CrossRef](#)]
51. Schmidt, S.B.; Husted, S. The Biochemical Properties of Manganese in Plants. *Plants* **2019**, *8*, 381. [[CrossRef](#)]
52. Guo, W.; Nazim, H.; Liang, Z.; Yang, D. Magnesium deficiency in plants: An urgent problem. *Crop. J.* **2016**, *4*, 83–91. [[CrossRef](#)]
53. Sega, D.; Baldan, B.; Zamboni, A.; Varanini, Z. FePO₄ NPs Are an Efficient Nutritional Source for Plants: Combination of Nano-Material Properties and Metabolic Responses to Nutritional Deficiencies. *Front. Plant Sci.* **2020**, *11*, 586470. [[CrossRef](#)] [[PubMed](#)]

54. Li, L.; Verstraeten, I.; Roosjen, M.; Takahashi, K.; Rodriguez, L.; Merrin, J.; Chen, J.; Shabala, L.; Smet, W.; Ren, H.; et al. Cell surface and intracellular auxin signalling for H⁽⁺⁾ fluxes in root growth. *Nature* **2021**, *599*, 273–277. [[CrossRef](#)] [[PubMed](#)]
55. Du, M.; Spalding, E.P.; Gray, W.M. Rapid Auxin-Mediated Cell Expansion. *Annu. Rev. Plant Biol.* **2020**, *71*, 379–402. [[CrossRef](#)]
56. Rayle, D.L.; Cleland, R. Enhancement of wall loosening and elongation by Acid solutions. *Plant Physiol.* **1970**, *46*, 250–253. [[CrossRef](#)]
57. Reuscher, S.; Akiyama, M.; Yasuda, T.; Makino, H.; Aoki, K.; Shibata, D.; Shiratake, K. The sugar transporter inventory of tomato: Genome-wide identification and expression analysis. *Plant Cell Physiol.* **2014**, *55*, 1123–1141. [[CrossRef](#)]
58. Shi, L.; Cao, S.; Shao, J.; Chen, W.; Zheng, Y.; Jiang, Y.; Yang, Z. Relationship between sucrose metabolism and anthocyanin biosynthesis during ripening in Chinese bayberry fruit. *J. Agric. Food Chem.* **2014**, *62*, 10522–10528. [[CrossRef](#)]
59. Das, P.K.; Shin, D.H.; Choi, S.B.; Park, Y.I. Sugar-hormone cross-talk in anthocyanin biosynthesis. *Mol. Cells* **2012**, *34*, 501–507. [[CrossRef](#)]
60. Jeong, S.W.; Das, P.K.; Jeoung, S.C.; Song, J.Y.; Lee, H.K.; Kim, Y.K.; Kim, W.J.; Park, Y.I.; Yoo, S.D.; Choi, S.B.; et al. Ethylene suppression of sugar-induced anthocyanin pigmentation in *Arabidopsis*. *Plant Physiol.* **2010**, *154*, 1514–1531. [[CrossRef](#)]
61. Peng, X.; Wu, H.; Chen, H.; Zhang, Y.; Qiu, D.; Zhang, Z. Transcriptome profiling reveals candidate flavonol-related genes of *Tetrastigma hemsleyanum* under cold stress. *BMC Genom.* **2019**, *20*, 687. [[CrossRef](#)]
62. Ding, Y.; Yu, S.; Wang, J.; Li, M.; Qu, C.; Li, J.; Liu, L. Comparative transcriptomic analysis of seed coats with high and low lignin contents reveals lignin and flavonoid biosynthesis in *Brassica napus*. *BMC Plant Biol.* **2021**, *21*, 246. [[CrossRef](#)] [[PubMed](#)]
63. Li, Y.; Xin, G.; Wei, M.; Shi, Q.; Yang, F.; Wang, X. Carbohydrate accumulation and sucrose metabolism responses in tomato seedling leaves when subjected to different light qualities. *Sci. Hortic.* **2017**, *225*, 490–497. [[CrossRef](#)]
64. Yoshida, T.; Anjos, L.D.; Medeiros, D.B.; Araujo, W.L.; Fernie, A.R.; Daloso, D.M. Insights into ABA-mediated regulation of guard cell primary metabolism revealed by systems biology approaches. *Prog. Biophys. Mol. Biol.* **2019**, *146*, 37–49. [[CrossRef](#)] [[PubMed](#)]
65. Balcke, G.U.; Bennewitz, S.; Bergau, N.; Athmer, B.; Henning, A.; Majovsky, P.; Jimenez-Gomez, J.M.; Hoehenwarter, W.; Tissier, A. Multi-Omics of Tomato Glandular Trichomes Reveals Distinct Features of Central Carbon Metabolism Supporting High Productivity of Specialized Metabolites. *Plant Cell* **2017**, *29*, 960–983. [[CrossRef](#)] [[PubMed](#)]
66. Li, D.; Li, L.; Luo, Z.; Mou, W.; Mao, L.; Ying, T. Comparative Transcriptome Analysis Reveals the Influence of Abscisic Acid on the Metabolism of Pigments, Ascorbic Acid and Folic Acid during Strawberry Fruit Ripening. *PLoS ONE* **2015**, *10*, e0130037. [[CrossRef](#)]
67. Hu, S.; Wang, F.Z.; Liu, Z.N.; Liu, Y.P.; Yu, X.L. ABA signaling mediated by PYR/PYL/RCAR in plants. *Yi Chuan* **2012**, *34*, 560–572. [[CrossRef](#)]
68. Zhao, H.; Nie, K.; Zhou, H.; Yan, X.; Zhan, Q.; Zheng, Y.; Song, C.P. ABI5 modulates seed germination via feedback regulation of the expression of the PYR/PYL/RCAR ABA receptor genes. *New Phytol.* **2020**, *228*, 596–608. [[CrossRef](#)]
69. Yuan, C.I.; Chaing, M.; Chen, Y.M. Triple mechanisms of glyphosate-resistance in a naturally occurring glyphosate-resistant plant *Dicliptera chinensis*. *Plant Sci.* **2002**, *163*, 543–554. [[CrossRef](#)]
70. Eberhard, J.; Bischoff, M.; Raesecke, H.R.; Amrhein, N.; Schmid, J. Isolation of a cDNA from tomato coding for an unregulated, cytosolic chorismate mutase. *Plant Mol. Biol.* **1996**, *31*, 917–922. [[CrossRef](#)]
71. Wu, M.; Xu, X.; Hu, X.; Liu, Y.; Cao, H.; Chan, H.; Gong, Z.; Yuan, Y.; Luo, Y.; Feng, B.; et al. *SIMYB72* Regulates the Metabolism of Chlorophylls, Carotenoids, and Flavonoids in Tomato Fruit. *Plant Physiol.* **2020**, *183*, 854–868. [[CrossRef](#)]
72. Wang, S.; Chu, Z.; Jia, R.; Dan, F.; Shen, X.; Li, Y.; Ding, X. *SIMYB12* Regulates Flavonol Synthesis in Three Different Cherry Tomato Varieties. *Sci. Rep.* **2018**, *8*, 1582. [[CrossRef](#)] [[PubMed](#)]
73. Ballester, A.R.; Molthoff, J.; de Vos, R.; Hekkert, B.; Orzaez, D.; Fernandez-Moreno, J.P.; Tripodi, P.; Grandillo, S.; Martin, C.; Heldens, J.; et al. Biochemical and molecular analysis of pink tomatoes: Deregulated expression of the gene encoding transcription factor *SIMYB12* leads to pink tomato fruit color. *Plant Physiol.* **2010**, *152*, 71–84. [[CrossRef](#)] [[PubMed](#)]
74. Lyu, J.I.; Park, J.H.; Kim, J.-K.; Bae, C.-H.; Jeong, W.-J.; Min, S.R.; Liu, J.R. Enhanced tolerance to heat stress in transgenic tomato seeds and seedlings overexpressing a trehalose-6-phosphate synthase/phosphatase fusion gene. *Plant Biotechnol. Rep.* **2018**, *12*, 399–408. [[CrossRef](#)]
75. O'Hara, L.E.; Paul, M.J.; Wingler, A. How do sugars regulate plant growth and development? New insight into the role of trehalose-6-phosphate. *Mol. Plant* **2013**, *6*, 261–274. [[CrossRef](#)] [[PubMed](#)]
76. Naikoo, M.I.; Dar, M.I.; Raghieb, F.; Jaleel, H.; Ahmad, B.; Raina, A.; Khan, F.A.; Naushin, F. Role and Regulation of Plants Phenolics in Abiotic Stress Tolerance. In *Plant Signaling Molecules. Role and Regulation Under Stressful Environments*; Khan, M.I.R., Reddy, P.S., Ferrante, A., Khan, N.A., Eds.; Woodhead Publishing: Sawston, UK, 2019; pp. 157–168.
77. Kou, X.; Yang, S.; Chai, L.; Wu, C.; Zhou, J.; Liu, Y.; Xue, Z. Abscisic acid and fruit ripening: Multifaceted analysis of the effect of abscisic acid on fleshy fruit ripening. *Sci. Hortic.* **2021**, *281*, 109999. [[CrossRef](#)]
78. Li, G.; Zhao, J.; Qin, B.; Yin, Y.; An, W.; Mu, Z.; Cao, Y. ABA mediates development-dependent anthocyanin biosynthesis and fruit coloration in *Lycium* plants. *BMC Plant Biol.* **2019**, *19*, 317. [[CrossRef](#)]
79. Ren, L.; Hu, Z.; Li, Y.; Zhang, B.; Zhang, Y.; Tu, Y.; Chen, G. Heterologous Expression of *BoPAP1* in Tomato Induces Stamen Specific Anthocyanin Accumulation and Enhances Tolerance to a Long-Term Low Temperature Stress. *J. Plant Growth Regul.* **2014**, *33*, 757–768. [[CrossRef](#)]
80. Mierziak, J.; Kostyn, K.; Kulma, A. Flavonoids as important molecules of plant interactions with the environment. *Molecules* **2014**, *19*, 16240–16265. [[CrossRef](#)]

81. Silva-Beltrán, N.P.; Ruiz-Cruz, S.; Cira-Chávez, L.A.; Estrada-Alvarado, M.I.; Ornelas-Paz, J.D.J.; López-Mata, M.A.; Del-Toro-Sánchez, C.L.; Zavala, J.F.A.; Márquez-Ríos, E. Total Phenolic, Flavonoid, Tomatine, and Tomatidine Contents and Antioxidant and Antimicrobial Activities of Extracts of Tomato Plant. *Int. J. Anal. Chem.* **2015**, *2015*, 284071. [[CrossRef](#)]
82. Martín-Rivilla, H.; García-Villaraco, A.; Ramos-Solano, B.; Gutiérrez-Manero, F.J.; Lucas, J.A. Improving flavonoid metabolism in blackberry leaves and plant fitness by using the bioeffector *Pseudomonas fluorescens* N 21.4 and its metabolic elicitors: A biotechnological approach for a more sustainable crop. *J. Agric. Food Chem.* **2020**, *68*, 6170–6180. [[CrossRef](#)]
83. Smith, C.A.; Want, E.J.; O'Maille, G.; Abagyan, R.; Siuzdak, G. XCMS: Processing Mass Spectrometry Data for Metabolite Profiling Using Nonlinear Peak Alignment, Matching, and Identification. *Anal. Chem.* **2006**, *78*, 779–787. [[CrossRef](#)] [[PubMed](#)]
84. Zhang, Y.; Li, Y.; Li, W.; Hu, Z.; Yu, X.; Tu, Y.; Zhang, M.; Huang, J.; Chen, G. Metabolic and molecular analysis of nonuniform anthocyanin pigmentation in tomato fruit under high light. *Hortic. Res.* **2019**, *6*, 56. [[CrossRef](#)] [[PubMed](#)]
85. Li, Y.; Chen, Y.; Zhou, L.; You, S.; Deng, H.; Chen, Y.; Alseekh, S.; Yuan, Y.; Fu, R.; Zhang, Z.; et al. MicroTom Metabolic Network: Rewiring Tomato Metabolic Regulatory Network throughout the Growth Cycle. *Mol. Plant* **2020**, *13*, 1203–1218. [[CrossRef](#)] [[PubMed](#)]
86. Yang, J.L.; Zhu, X.F.; Peng, Y.X.; Zheng, C.; Ming, F.; Zheng, S.J. Aluminum regulates oxalate secretion and plasma membrane H⁺-ATPase activity independently in tomato roots. *Planta* **2011**, *234*, 281–291. [[CrossRef](#)] [[PubMed](#)]